VFAST Transactions on Software Engineering
https://vfast.org/journals/index.php/VTSE@ 2024, ISSN(e): 2309-3978, ISSN(p): 2411-6246
Volume 12, Number 3, July-September 2024 *pp:147-165*

X-ray Image Analysis for Dental Disease: A Deep Learning Approach Using EfficientNets

Muhammad Adnan Hasnain [1], **Zeeshan Ali** [1*], **Muhammad Sajid Maqbool** [2], **Musfira Aziz** [3]

[1]Department of Information Engineering and Computer Science and Mathematics, University of L'Aquila, Italy; [2]Department of Computer Science, NFC Institute of Engineering and Technology, Multan, Pakistan; [3]Department of Computer Science, National College of Business Administration and Economics Lahore, Pakistan

Keywords: *Dental Disease, Dentistry, Dental Caries, Medical Imaging, CNN, Deep Learning, Machine Learning*

Journal Info:
Submitted:
September 17, 2024
Accepted:
September 18, 2024
Published:
September 22, 2024

Abstract Dental cavities are a highly common persistent dental problem that impacts populations across different age groups on a global scale. It is crucial to get a dental issue diagnosed as early as possible and with as much accuracy as possible to treat it efficiently and prevent any related issues. If a dental infection is not treated, it will eventually grow and cause tooth loss. Dental X-ray images are crucial and beneficial in the diagnostic process of dental diseases for dentists. By applying Deep Learning (DL) techniques to dental X-ray images, dental experts can efficiently and precisely detect dental conditions, including dental cavities, fillings and implants. The objective of this research is to assess the performance of DL-based methods for dental disease detection via panoramic radiographs. In this study, we evaluated the performance of all of the EfficientNet variants (e.g., EfficientNets B0-B7) to determine which one is the most effective model for detecting dental disease. Moreover, we utilized the Borderline Synthetic Minority Oversampling Technique (SMOTE) to cope with the issue related to the minority classes contained in the dataset. To assess the efficacy of the model, various metrics are employed, including recall, accuracy, precision, loss, and F1-score. As a result, the performance of the EfficientNet-B5 model was superior to that of the other EfficientNet models. The EfficientNet-B5 model achieved the following values for its metrics: F1-score, accuracy, recall, AUC, and precision: 98.37%, 98.32%, 98.32%, 99.21%, and 98.32%, respectively. The accuracy rates for the EfficientNet-B0, EfficientNet-B1, EfficientNet-B2, EfficientNet-B3, EfficientNet-B4, EfficientNet-B6, and EfficientNet-B7, are 91.59%, 94.12%, 93.28%, 85.71%, 94.96%, 96.64% and 90.76%, respectively. The results indicated that the EfficientNet-B5 model performs better than other EfficientNet classifiers, which supports dental professionals significantly in the recognition of dental diseases.

***Corresponding author email address:** zeeshan.ali@graduate.univaq.it
DOI: 10.21015/vtse.v12i3.1912

1 Introduction

Dental cavities are a widespread and chronic infectious dental problem that affects people of all ages worldwide. It is estimated that almost 50% of the population is impacted by the current prevalence of dental disease, with permanent cavities impacting 2.3 billion individuals [1], [2], [3]. Caries, also known as cavities or tooth decay, is a dental condition that is characterized by the production of lactic acids by bacteria found in the mouth, which cause damage to the enamel layer of the affected tooth. This could potentially result in the formation of small cracks among the teeth, which, if left untreated, could result in infection, discomfort, and tooth loss [4], [5], [6]. In addition, it is noteworthy that in the Republic of Korea in the year 2020, dentists treated over 6 million patients who had dental cavities, and of these 1.45 million were kids aged 0 to 9 years [7]. Therefore, the treatment of dental cavities disease presents a challenge for scientists. Cavities in the teeth are a form of tooth decay that can be initiated by particulates of food that remain on the teeth after a meal has been consumed and can be a threat to oral health. Teeth may become weaker and porous, or they can break as a result of this condition.

Dental information technologies are an emerging discipline within an area of dentistry that has the potential to improve and extend the processes of analysis in dental practices, save patients time as well as relieve the stress they encounter daily [8]. The most common oral diseases that affect the standard of living are dental diseases [3],[9]. However, according to a prior Korean study, just 21% of the population visits its dental hospitals and clinics for their dental checkups [10]. All people, even children, who have teeth are vulnerable to cavities. If cavities are not treated, they will continue to spread into deeper parts of our teeth and become more severe. The most effective method for protection against cavities is to maintain a routine for dental care. This should involve going to the dentist for regular checks as well as washing and brushing your teeth regularly. The symptoms associated with cavities can vary significantly, depending upon the cavities' position and degree of severity. During the beginning phases of cavity growth, there is a chance that you won't notice any symptoms at all. Symptoms that can appear as the process of cavities develops include toothache, or sudden pain, tooth sensitivity, and a mild to severe disease induced by consuming sweet, warm, or frozen substances. brown, white, or black darkening on any portion of a tooth, and pain caused after biting up [10]. By treating a cavity before the beginning of pain, the possibility of tissue damage is decreased, thereby conserving a greater portion of the tooth structure [11].

Dental professionals are responsible for detecting problems associated with teeth. A dentist may take X-rays, inquire about pain, and examine the teeth in order to detect cavities early. The lesions caused by dental cavities might not all be detectable with a visual or touchable examination. As a direct consequence of this, imaging approaches are commonly used to enhance the rate of identification [12], [13], [14]. In past years, medical imaging methodologies, which include X-rays, have been of great assistance in the diagnosis and treatment of numerous diseases [15]. X-ray technology has facilitated the detection of dental diseases by dental clinicians. Dental radiographs can be classified as either extra-oral or intra-oral. Periapical and bitewing X-rays are intraoral radiographs that can image specific parts of the mouth and necessitate multiple examinations to capture distinct areas. This takes a lot of time to analyze, makes the patient irritated, and can increase the amount of radiation consumed [16].

For this study, extra-oral radiographs (such as panoramic X-ray images) have been chosen due to their superior performance compared to conventional radiograph imaging methods. Using a single X-ray, they illustrate (i) the entirety of the oral cavity, (ii) every tooth in the upper and lower mandible, and (iii) the locations of both fully emerged and emerging teeth. Additionally, it is well-suited for the field of dentistry due to its expedited treatment time, increased ability to diagnose, reduced radiation consumed, and ease of infection control procedures [17]. Panoramic X-ray imaging is an excellent option to identify dental issues due to its low cost and relatively low radiation requirement [18]. Time and expertise are required for manual examination of dental issues to categorize

and identify dental diseases. However, the manual procedure for evaluating dental diseases is laborious and susceptible to error when performed by dentists lacking experience [17]. In this case, researchers have implemented various advanced Machine Learning (ML) and DL architectures, to automatically diagnose dental diseases through the use of X-ray images. A little progress has been made toward the automatic detection of dental issues [17]. The success of the treatment and diagnosis is thus reliant on the capabilities of the reading expert as well as technological advancements [19]. The implementation of an automated system for detecting and classifying dental issues may prevent the loss of teeth and assist in the early detection of disease.

The type of artificial neural networks (ANNs) known as DL has made significant advances and is effectively used in computer vision applications such as object detection, tracking, face and activity identification, and multidimensional mapping and localization [20], [20]. In 2006, Hinton presented the idea of DL to the scientific community as an improved version of multilayer ANNs [21]. Additionally, DL-based CNN approaches for the identification and categorization of diabetic retinopathy, pulmonary tuberculosis, and skin cancer have already proven to be highly accurate and effective, with encouraging clinical applications [22], [23]. A selection of labelled datasets and neural network layers are employed to train the model. However, the advantage of existing DL-based approaches is that they automatically use learning to extract important features from images [24].

In medical images, the most popular technique for classifying, identifying, and segmenting organs or diseases is convolutional neural networks, or CNNs [25], [26], [23]. CNN is one of the most widely utilized and popular DL networks. Currently, DL is extremely prominent due to CNN. CNN's primary advantage over its predecessors is that it detects significant features automatically and without human intervention, which has led to its popularity. The CNN architecture comprises the fundamental components, which consist of fully connected layers, convolution layers, and pooling layers [27], [28]. A fundamental element of the CNN architecture, the convolution layer performs the extraction of features. This process generally involves a combination of nonlinear and linear operations, specifically the process of convolution and activation function [29].

In dentistry, DL has become a significant topic, specifically in the detection of dental caries [30], [31]. However, because there haven't been a lot of studies conducted regarding dental categorization using DL, this is still a topic that requires more investigation within the field [32]. Consequently, the purpose of this study is to assess the performance of EfficientNet variants (such as EfficientNet B0-B7) for dental disease detection by using X-ray images and these models can recognize the three different categories of dental diseases such as dental cavities, fillings, and implants. The following are the primary contributions of the research:

1. In this present study, EfficientNets B0-B7 models were evaluated to examine which one model might be most suitable for the detection of dental disease.
2. The accuracy of the models is affected as a result of the problem of class imbalance that happens within the dataset. We utilized the BL-SMOTE oversampling approach, which adds new images to balance the class samples so that we tackle the imbalance problem that was present in the dataset.
3. By employing the Grad-CAM heat-map algorithm, the class activation map is visually represented, emphasizing the characteristics that contribute to the categorization of a given image sample.
4. In comparison to the other EfficientNet architectures, the EfficientNet-B5 architecture achieved superior results across a variety of evaluation criteria, including recall, F1-score, accuracy, recall, precision, AUC, and loss.

The subsequent portions of the paper are structured according to the mentioned categories. A description of the literature review is found in Section 2. We explained the methodology in Section 3. The discussion and results are provided in Section 4, and the study is concluded in Section 5.

2 Literature Review

A significant number of research has been given to the detection of dental diseases to aid dental professionals in identifying the condition at an early stage. The results of recent studies regarding the application of DL and ML models for the detection of dental disease are outlined in the Table 1. An enhanced approach was devised by Kang et al[7] to identify cases of decaying teeth that may pose a health risk. By combining the mRMR + GINI choosing features and the GBDT algorithm, they were able to design a method that would enhance the detection of dental caries. An assessment of performance was conducted utilizing the five ML classifiers (LR, RF, SVM, LSTM, and GBDT) that served as the benchmarks. The proposed GBDT classifier, which was built with a more limited feature set than the other classifiers that were discussed, displayed the most successful classification outcome. The researchers built their dataset with the 2018 Children's Teeth Survey conducted by the Korea Institutes for Disease Prevention and Control as the basis for their work. The following are the values that were achieved for accuracy, precision, recall, and F1-score: 95%, 98%, 88%, and 93%, respectively. Ali et al [33] employed Google BERT for semantic feature extraction, which has proven to be an effective technique for capturing contextual representations and MLP for training the Deep Learning model for the classification tasks. Based on the VGG16 model, Kalita et al[34] suggested the fine-tuned model. Their model classified dentin cavities using simulation-based methods. A collection of Radio Visio Graphy (RVG) images depicting weakened teeth was acquired and annotated to conduct their research. Additionally, a comparative analysis was conducted between the model they provided and the fully developed VGG16 and the Bi-LSTM paired via transfer learning. 550 tooth periapical RVG photographs were acquired of individuals ranging in age from 18 to 70 years; photos were collected from this group.In comparison to the completely developed model, the proposed approach demonstrates superior performance, attaining an accuracy of 97.87% and a loss of simply 0.0325 throughout 20 iterations. A technique proposed by Haghanifar et al [35] for autonomously identifying tooth caries in panoramic images was presented. Their technique applies a network of capsules to determine outcomes for estimation, and utilizes numerous deeper models learned through transfer learning to obtain meaningful data. Their algorithm used a collection of images comprising 470 panoramic images and was able to achieve an accuracy of 86.05% on the set that was tested. For extreme and moderate serious situations, their model yielded recall rates of 90.52% and 69.44%, respectively. They confirmed that severe cavity regions were quicker to identify and that a larger dataset is needed to achieve effective moderate cavity recognition.

Chen et al[36] devised a detection method that concurrently identified tooth decay and periodontitis by applying DL and image processing strategies to dental X-ray photographs. Using the YOLOv7 object identification method, the single-tooth X-ray photo is identified and subsequently edited using the periapical X-ray image. After that, an adjustment was made to the regional intensity utilizing a technique known as brightness-limited equalization of histograms utilizing adaptive algorithms. The DL framework that is being used for classification is constructed of layers that are completely coupled to one another and a recently learned EfficientNet-B0. To overcome the difficulties associated with detection, the sigmoid function is employed to produce two labels. When it comes to tooth detection, the YOLOv7 algorithm has a precision rating of 97.10% on average.

Fatima et al [37] designed an automatic model that was constructed using two separate components. The initial component was a modified and lightweight MobileNet-v2 that leveraged a region-based network (RPN) to assess periapical diseases on an initial dataset. In the initial stages, a series of visual observations received preprocessing to eliminate noise, increase contrast, and improve image quality. The researchers then derive features from the preprocessed images using the lightweight technique they have suggested. The retrieved feature maps are subsequently transmitted to the RPN, where they are utilized in the creation of region proposals. The region vector unit for the

region of interest (ROI) is subsequently provided with these region proposals. After the concurrent processing of the region proposals and the visualization of features, this block classifies the incoming image using FCLs. Panyarak et al [38] evaluated the viability of classifying tooth decay by employing bitewing radiography and DL techniques. To assess the performance of ResNet-50, ResNet-101, ResNet-18, and ResNet-152, an entire set of 2758 annotated bitewing radiographs were arbitrarily divided into three distinct research studies. To assess the effectiveness of each technique, a study was conducted on both the results of the vectors and the AUC curve. The experimental results demonstrated that ResNet-50 attained the maximum level of accuracy 75.00%, after which came ResNet-101 at 74.09%, in that particular order. In the classification dental caries regarding the ICCMSTM-RSS, the performance of the ResNet models was approximately average. A dental disease segmentation architecture known as the Dental Caries Detection Network (DCDNet) was proposed by Dayı et al[39].

This segmentation design is primarily distinguished from others of its sort by the Multi-Predicted Outcome architecture situated in the last part of DCDNet. To identify occlusal, proximal, and apical tooth decay, the ultimate feature map in MPO was split into three separate routes. A series of exhaustive experimental evaluations were conducted to assess the functionality of the DCDNet architecture. The image collection parameters utilized for radiographs using the Planmeca Promax 2-D Panoramic System were as follows: 14 mA, 12 seconds, and 68 kVp. Labels were applied to 504 panoramic radiography images utilized in the experimental trials to denote the presence of 378 apical tooth decay, 746 occlusal tooth decay, and 1627 closer tooth decay, respectively. As a form of AI, Hasnain et al [40] applied DL to diagnose dental conditions through the evaluation of images from X-rays. The set of photos consists of 126 images, all of which have been assessed as Normal or Affected by tooth specialists. To enhance the efficacy of DL structures throughout the development process, data augmentation is executed to augment the dataset in size.

To verify the authenticity of an image and detect abnormalities, a CNN architecture is constructed in its entirety. Their architecture includes the following layers: max-pooling, convolutional, flatten, dense, and output. To automate the assessment of healthcare quality of services, an augmented reality (CNN) model is constructed employing the supplementary data. To evaluate the effectiveness of the model, several distinct metrics are employed, such as accuracy, recall, loss, precision, and F1-score. Oztekin et al [41] conducted a comparison to decide which of three renowned models, including EfficientNet-B0, ResNet-50, and DenseNet-121, which had already been developed, executed the cavity recognition task most efficiently. The approaches take panoramic photos as input and create a heat map that illustrates spots of concern on the tooth surface, in addition to a classification that determines whether a tooth has caries or does not have caries. The effectiveness of the framework that they built was evaluated by deploying full panoramic photos that included 562 individuals as subjects. The three models' conclusions were quite similar to one another.

However, the outcomes of the ResNet-50 model were demonstrated to be significantly better than those of the EfficientNet-B0 and DenseNet-121 methods. After further investigation, it was found that the heat maps were additionally situated in areas that were known to contain cavities. Karaoglu et al[42] devised the heuristic algorithm-based approach known as Mask R-CNN, which was verified through the analysis of panoramic radiographs of the teeth. The initial author, DentiAssist, a web-based labelling system, was employed by two dental radiologists to perform the ground-truth categorization of images necessary for the development of the DL technique. The dataset was compiled using 2702 tooth images from which the identifying information had been extracted. The dataset is divided into three sections: labelled the training set, the validation set, and the test set comprising 1747, 484, and 471, images, respectively. The investigation yielded the following results regarding the corresponding percentages

of a f1-score and accuracy: 95.87%, and 92.49%, respectively. Jiang et al [43] proposed a two-stage DL architecture comprised of YOLO-v4 and UNet for discriminating critical locations and the dental pulp.

To precisely measure the amount of gingival bone loss in the alveolars and to diagnose periodontitis, this procedure was executed. The model's ability to recognize these traits was evaluated, and the outcomes were compared to those of beginner dental professionals. An overall of 640 panoramic images were utilized in the study. Three efficient gum specialists were tasked with identifying the critical areas necessary for quantifying the extent of gingival dental bone loss, as well as the specific location and structure of alveolar tooth loss. In their study, AL-Ghamdi et al [40] offered a CNN capable of performing multipurpose segmentation. This is achieved by classifying X-ray images into three separate groups: filling, cavity, and implant. CNN was presented in the context of a NASNet architecture in their paper, which featured a variety of dropout layers, max-pooling layers, and activating functions in different quantities. Following the initial preprocessing and enhancement of the data, the next step procedure involved the construction of a multiple-outcome method. Ultimately, a framework was created and formulated; the loss and accuracy metrics served as the evaluation parameters for the model's analysis. After a limited number of alterations, the model's accuracy surpassed 96%. Muramatsu et al [44] developed a computerized method for classifying and identifying teeth in dental panoramic views to automate the systematic filing of dental records.

Furthermore, it served as a preliminary stage in the process of image preparation that preceded the computerized evaluation of dental diseases. The fourfold cross-validation method was applied to the development and assessment of a system for object detection utilizing a total of one hundred panoramic dental scans. After the identification of bounding frames, a classification system was implemented to classify them into one of four dental types—molars, premolars, incisors, and canines—and three dental nations—completely restored, partially restored, non-metal restored, and fully restored.In consideration of the visualization outcome, a CNN's double initial stages were constructed using a variety of image data of various sizes.

Muresan et al[45] developed an innovative approach to classify dental issues and autonomously identify teeth utilizing panoramic X-rays. The primary objective of their approach was to aid healthcare providers in making informed decisions regarding the most suitable course of treatment. To elucidate fourteen distinct dental issues that may appear, panoramic radiographs were acquired from three distinct dental treatments, documented, and interpreted as part of their research. In the initial stages of training a CNN to acquire information about semantic segmentation, the data was supplemented with annotations.

Subsequently, a variety of image processing techniques were implemented to further refine and separate the bounding frames associated with the dental identifications. Ultimately, a unique identifier was assigned to each dental incident, and the affecting issue was determined employing a histogram-based vote of the majority method within the identified zone of concern. The prediction model proposed by Kang et al[46] for dental caries was the DCP, which comprises three components: data acquisition, data prepossessing, and the estimation model. Predicting the presence or missing cavities in children, the proposed DCP model, which consists of ML and DL models, utilizes features extracted from the preprocessed data acquired from the survey. Age, region, gender, and other characteristics are included in a labelled dataset comprising 22,287 samples. Their performance was assessed using accuracy, F1-score, precision, and recall when combined with several ML algorithms that were applied to this data. In comparison to other ML approaches, random forest has demonstrated the maximum level of performance, attaining an F1-score of 90%, accuracy of 92%, precision of 94%, and recall of 87%.

The MMDCP (Multi-Modal Dental Caries Prediction) approach, as proposed by Ngnamsie Njimbouom et al [47], comprises three distinct phases: collecting data, preprocessing of data, and the prediction module. Multiple sources contributed to the multimodal

dataset utilized by the model. After the initial phase, where the two datasets have been processed independently, a combination of algorithms (DenseNet201 and ANN) was applied to the preprocessed data. To gain observations from the cross-modality combined heterogeneous characteristics present in the dataset, the two neural networks were combined. The performance of the proposed predictor approach, which was built utilizing multi-modal data, was extremely encouraging, achieving 89% F1-score, 90% recall, 90% accuracy, and 89% precision. A CNN proposed by Lian et al. citeplian2021deep, known as nnU-Net, used to identify cavities lesions. To classify the lesions based on their depths (specifically, dentin spots in the outside, center, or inside part D1/2/3 of dentin), DenseNet121 was implemented.

The assessment of 1160 tooth panoramic images was conducted by three dental professionals. Circular marks were used to indicate all caries lesions in the radiographs; the combination of these marks served as the reference dataset. Subsequently, a validation and training set (1071) and a test set (89) were derived from the initial set. Six expert dental professionals' evaluations were utilized to evaluate the efficacy of the test data in the trained nnU-Net and DenseNet121 methods with the metrics of Dice coefficient, intersection over union (IoU), precision, negative predictive value (NPV), accuracy, recall, and F1-score.

3 Materials and Methods

This section provides an in-depth description of each phase that has been performed. The collection of data is the first step in the procedure, and then the Borderline (BL-SMOTE) technique is applied in the next phase. In the third phase, the experimental methodology employed to assess the performance of EfficientNet models is provided.

3.1 Dataset Description

Dental panoramic X-rays were taken from the Nishtar Institute of Dentistry, which resides in Multan, Pakistan. Within the private collection, there are a total of 549 images that depict patients who are afflicted with dental disorders. Specifically, these are dental cavities, fillings, and implants. Figure 1 depicts the number of

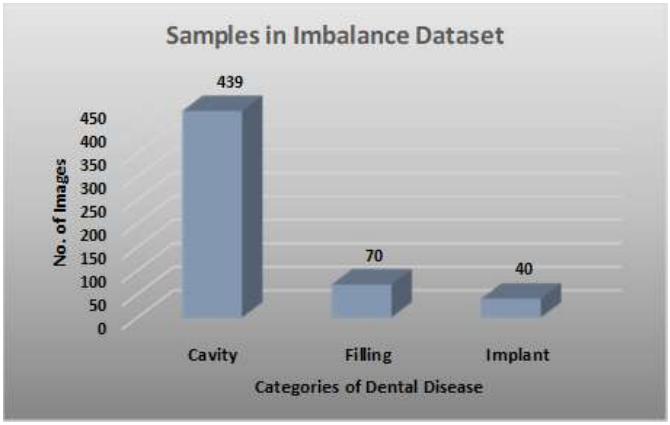

Figure 1. Distribution of classes in dental datasets before up-sampling

dental disease samples that were divided up before the upsampling and Figure 2 displays the samples of dental disease images.

3.2 Applying BL-SMOTE to Balance Every Class Sample

We implement the up-sampling procedure for tackling the problem of unequal class distribution within the dataset. Up-sampling is the method of including additional zero-valued data in between the initial samples to improve the sampling rate. Using this method, we employ an up-sampling technique named BL-SMOTE for producing fusion examples for every class [49]. Employing this approach, an evaluation of the minority class is the first step in the classification process. When generating data that is synthetic, any minority analysis is classified as noise and avoided if every neighbour is part of the majority category. Furthermore, it replicates just a small amount of border neighbourhoods that are linked to both minority and majority samples. Figure 3 illustrates the sample allocation after the implementation of the BL-SMOTE approach.

3.3 Proposed Classification Method

One of the most significant dental issues is cavities in the teeth, which are becoming more widespread in individuals of every age, including children. Patients with dental cavities need to obtain treatment that is both efficient and quick to decrease their level of suffering. The infection caused by bacteria will grow and may re-

Table 1. Recent research utilizing ML and DL Models to Diagnose Dental Diseases

Reference	Publication Year	Models	Diagnostic Technique	No. of Images	Accuracy
[7]	2023	GBDT, RF, LR, SVM, LSTM	Dental Images	20,593	95.19%
[35]	2023	CNN	Panoramic Radiographs	470	86.05%
[36]	2023	EfficientNet-B0	Periapical Radiographs	1,525	95.44%
[37]	2023	MobileNet-v2	Periapical Radiographs	534	93%
[38]	2023	ResNet-50 and ResNet-152	Bitewing Radiographs	2,758	75.00%
[39]	2023	DCDNet	Panoramic Radiographs	504	75.93%
[41]	2023	EfficientNetB0, DenseNet121, ResNet50	Panoramic Radiographs	13,870	92%
[42]	2023	Mask R-CNN	Panoramic Radiographs	2,702	92.49%
[43]	2022	YOLO-v4 and UNet	Panoramic Radiographs	640	77%
[40]	2022	NASNet, AlexNet, and CNN	Panoramic Radiographs	245	96.51%
[46]	2022	Random Forest	Dental Images	22,287	92%
[47]	2022	DenseNet201	Dental Images	22,371	90%
[44]	2021	CNN	Panoramic Radiographs	100	93.20%
[48]	2021	DenseNet121	Panoramic Radiographs	1,160	95.70%
[45]	2021	CNN	Panoramic Radiographs	1,000	89%

sult in tooth loss if treatment is not provided. It is possible to prevent tooth loss as long as this condition is recognized and treated promptly. This study presents DL models through the use of panoramic dental images to identify between fillings, implants, and cavities. The CNN-based EfficientNet B0-B7 [50] models were used for the classification process and Figure 4 shows the block diagram for this study.

The image dimension's range is fixed at 150 × 150 pixels and the initial processing of the image collection involved normalization. The values in the 0–1 range have been adjusted to make the dataset easier for the model to understand. Three distinct groups have been created from the dental disease dataset: testing, validation, and training. 80% of the dataset is used as training data, 10% is employed for a testing purpose, and 10% is used for validation. Subsequently, a technique known as BL-SMOTE is implemented to address the problem related to the uneven data set. To equalize the dataset, this algorithm oversamples

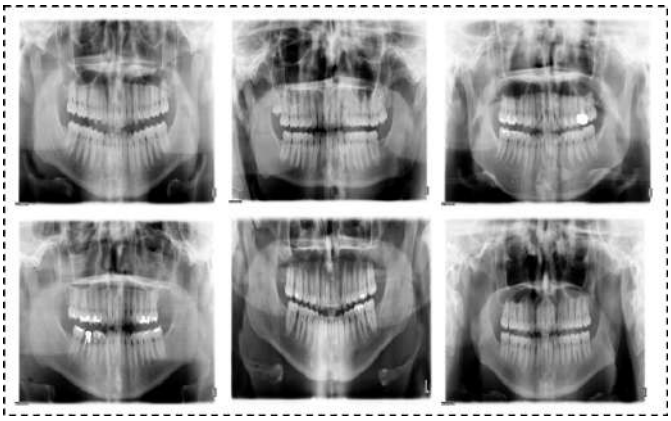

Figure 2. Sample Images of Dental Dataset

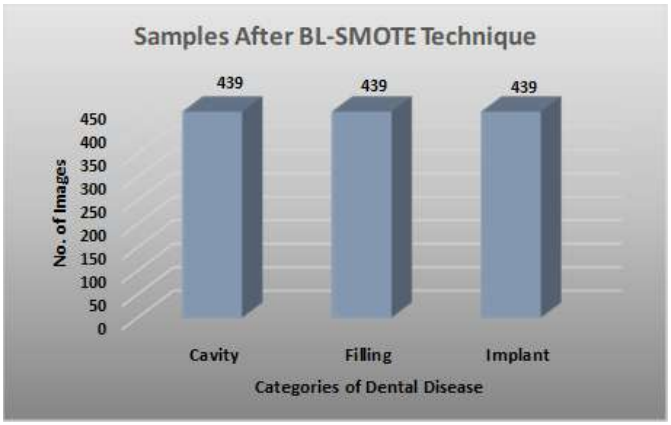

Figure 3. Distribution of classes in dental datasets after up-sampling

the categories. A total of thirty epochs in all were conducted with the experimental approach. After completing every epoch, the EfficientNet models have reached the required level of accuracy for validation and training. The same hyper-parameters were used to train EfficientNetB0-B7 models to identify the optimal model. The "compound scaling" concept is the foundation of the EfficientNet model. The concept of compound scaling is based on scaling three primary aspects of a neural network such as depth, width, and resolution. The total amount of layers in the structure is associated with depth scaling. Resolution scaling entails changing the size of the input image, whereas width scaling relates to the amount of channels in every layer of the neural network. In EfficientNet, inverted residual blocks and depth-wise separable convolutions are used to create Mobile Inverted Bottleneck (MBConv) layers. An essential component of the EfficientNet architecture is the MBConv layer. With a few modifications, it is designed using the inverted residual blocks from MobileNetV2. The depth-wise convolution in the MBConv layer is the first step, and it is subsequently followed by a point-wise convolution (1x1) that increases the number of channels and an additional convolution (1x1) which decreases the number of channels back to the initial value. The bottleneck structure maintains the model's representational power high while allowing efficient learning [50].

There are several versions of EfficientNet with different scaling coefficients, including EfficientNet-B0, EfficientNet-B1, EfficientNet-B2, EfficientNet-B3, and so on. Users can choose the best model version for their particular needs by considering the various trade-offs among model size and accuracy that each variant represents. However, there are 237 total layers in EfficientNet-B0 and 813 total layers in EfficientNet-B7, each of these layers is composed of five modules. Any EfficientNet network starts with its stem, which is the same for all eight models. After this, there are seven blocks in each of them. As we proceed from EfficientNetB0 to EfficientNetB7, the number of sub-blocks within these blocks also varies. The only thing that separates these architectures is the variation in the number of feature maps (channels), which raises the total number of parameters.

3.4 Model Evaluations

A confusion matrix was applied in this study to make sure the model's effectiveness could be assessed. The dataset was initially split into training and test samples before the model was created. The test data was subsequently utilized to verify the accuracy of the architecture. To determine the model's effectiveness, we utilized several different measures. The following evaluation metrics (see Equations (1) – (8)) are frequently used to determine how well the EfficientNet models detect dental diseases:

$$\text{Accuracy} = \frac{TP + TF}{TP + TN + FP + FN} \quad (1)$$

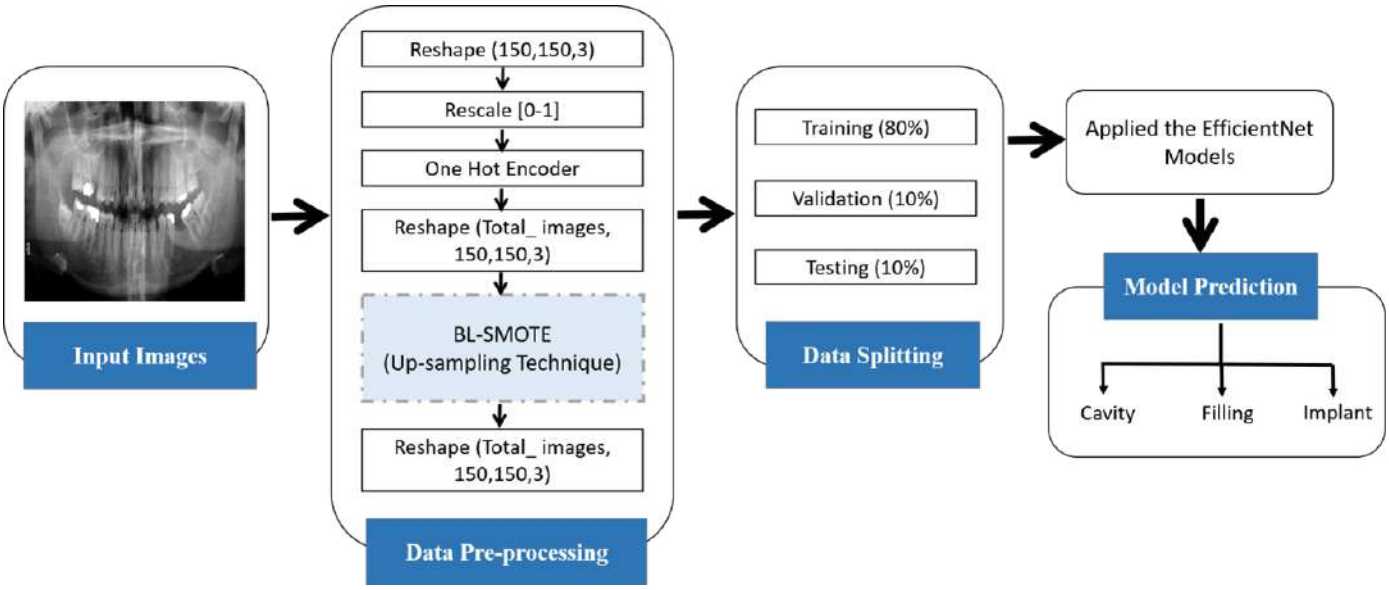

Figure 4. A block diagram displaying the techniques used in this study

$$\text{Precision} = \frac{TP}{TP + FP} \tag{2}$$

$$\text{Recall} = \frac{TP}{TP + FN} \tag{3}$$

$$\text{F1-Score} = 2 * \frac{\text{Precision} * \text{Recall}}{\text{Precision} + \text{Recall}} \tag{4}$$

$$\text{FPR} = \frac{FP}{FP + TN} \tag{5}$$

$$\text{TPR} = \frac{FP}{FP + FN} \tag{6}$$

$$\text{Loss} = y - \bar{y} \tag{7}$$

$$L_{CE} = -\sum_{n=1}^{k} \left(L_i \log(p_i)\right) \tag{8}$$

4 Results and Discussion

The results of this study, which were used to assess the performance of the models, are explained in this section and these models are included from EfficientNet-B0 to EfficientNet-B7. We will compare the models that have been provided in this section.

Table 2. A list of the hyper-parameters that are used in the EfficientNet Models

Hyper-parameter	Type
Batch Size	32
Optimizer	RMSprop
Learning Rate	0.001
Call back	ReduceLROnPlateau
Epochs	30

4.1 Experimental Setup

A Windows 10 PC configured with an 11 GB NVIDIA GPU and 32 GB RAM was employed to conduct the research study. The EfficientNet models utilize x-ray imaging data to identify three distinct types of dental disease such as cavity, implant, and filling. Furthermore, the keras library has been used to implement an EfficientNet classifier, and the Python language has made it possible to implement approaches. Table 2 describes the hyper-parameters that are essential to the EfficientNet model's performance.

4.2 Evaluation of EfficientNet Models using Accuracy

To increase the number of samples for classes with fewer images, the BL-SMOTE method is applied to the

dataset. This eventually led to the expansion of the data set from 549 samples to 1317 distinct instances, as previously stated. Consequently, the problem of unequal data distribution is resolved. The EfficientNet Models, EfficientNet-B0, EfficientNet-B1, EfficientNet-B2, EfficientNet-B3, EfficientNet-B4, EfficientNet-B5, EfficientNet-B6, and EfficientNet-B7, obtained accuracies of 91.59%, 94.12%, 93.28%, 85.71%, 94.96%, 98.32%, 96.64%, and 90.76%, respectively, based on the results shown in Table 3. Figure 5 illustrates the substantial enhancement that the EfficientNet-B5 model achieved in comparison to EfficientNet B0-B1-B2-B3-B4-B6-B7. The EfficientNet-B5 model has been appropriately trained and operates well on the test dataset, even though the model's poor accuracy at epoch 1 and improvement as epochs increase. Epochs were plotted on the x-axis and accuracy was on the y-axis of the accuracy graph.

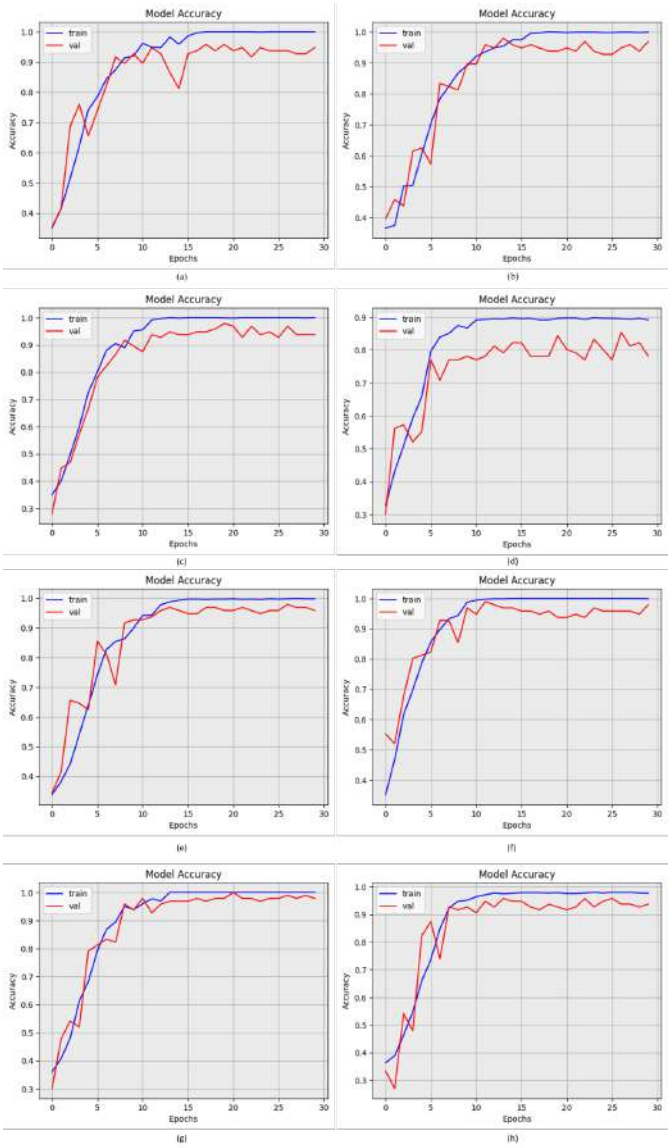

Figure 5. Accuracies of the EfficientNet Models; (a) EfficientNet-B0, (b) EfficientNet-B1, (c) EfficientNet-B2, (d) EfficientNet-B3, (e) EfficientNet-B4, (f) EfficientNet-B5, (g) EfficientNet-B6, (h) EfficientNet-B7.

4.3 Loss of the EfficientNet Models

A loss function evaluates the rate at which a neural network predicts the training set of data by comparing the desired and predicted value of the output. The aim during training is to reduce this loss between the target and expected outcomes. The term "categorical cross-entropy" refers to a cross-entropy technique that addresses a categorization problem involving numerous classes by utilizing a loss function. Loss functions are constructed to determine the degree of estimates required to differentiate the actual value from the expected one. The EfficientNet Models such as EfficientNet-B0, EfficientNet-B1, EfficientNet-B2, EfficientNet-B3, EfficientNet-B4, EfficientNet-B5, EfficientNet-B6, and EfficientNet-B7, obtained loss values of 0.3996, 0.3705, 0.3592, 0.4231, 0.2645, 0.1364, 0.2037, and 0.2513, respectively, based on the results shown in Figure 6, demonstrates that the EfficientNet-B5 model's loss value is significantly reduced as compared to that of the EfficientNet B0-B1-B2-B3-B4-B6-B7 model.

4.4 Analysis of EfficientNet Models Using ROC & ROC's Extension

A ROC is a plot that serves to illustrate the possible connection between sensitivity and specificity for all feasible thresholds for a set of experiments. The experiment's sensitivity, which is represented on the vertical axis of the ROC curve plot, correlates with its specificity, which is represented on the horizontal axis of the plot. While sensitivity shows how many positive outcomes there are in a particular sample, 1-specificity evaluates the quantity of false positives. The performance of the binary or multi-classifier is the main

Table 3. Comparative analysis of all EfficientNet Models (B0 - B7)

Classifiers	Precision	Accuracy	Recall	AUC	F1-Score
EfficientNet-B0	91.59%	91.59%	91.59%	97.78%	91.59%
EfficientNet-B1	94.12%	94.12%	94.12%	97.81%	94.14%
EfficientNet-B2	93.28%	93.28%	93.28%	97.76%	93.29%
EfficientNet-B3	86.84%	85.71%	83.19%	94.65%	85.19%
EfficientNet-B4	94.96%	94.96%	94.96%	98.28%	94.76%
EfficientNet-B5	98.32%	98.32%	98.32%	99.21%	98.37%
EfficientNet-B6	96.64%	96.64%	96.64%	98.43%	96.47%
EfficientNet-B7	90.76%	90.76%	90.76%	97.85%	90.20%

focus of the ROC analysis, which is additionally employed to assess the efficacy of the diagnostic tests. A classifier's performance is estimated by employing the area under the curve (AUC) of the ROC; an increased AUC denotes a more efficient classifier. Based on the results shown in Figure 7, the EfficientNet Models, namely EfficientNet-B0, EfficientNet-B1, EfficientNet-B2, EfficientNet-B3, EfficientNet-B4, EfficientNet-B5, EfficientNet-B6, and EfficientNet-B7, obtained ROC values of 98.12%, 96.85%, 98.12%, 96.86%, 97.73%, 98.53%,97.73%, and 96.39%, respectively. Figure 7 illustrates the substantial enhancement that the EfficientNet-B5 model achieved compared to the EfficientNet B0-B1-B2-B3-B4-B6-B7 model. Using an extension of the ROC curve, Figure 8 shows the performance of EfficientNet models (B0-B7). Dental disease can be classified into three categories: category 0 (cavity), category 1 (filling), and category 2 (implant).

4.5 Confusion Matrix of EfficientNet Models

An algorithm for classifying data is defined through the use of a confusion matrix. The performance of a classification algorithm is summarized and represented using a confusion matrix. The confusion matrix, which is produced by mapping the expected results to the predicted results of an algorithm, provides a structured method for learning additional information about a classification algorithm. The substantial increase in efficiency that the EfficientNet-B5 model attained compared to the EfficientNet B0-B1-B2-B3-B4-B6-B7 model is depicted in Figure 9.

Furthermore, we employed the Grad-CAM heat-map approach to generate a graphical depiction of the results attained by the EfficientNet-B5 model. The heat map's main objective is to emphasize the portion of the mouth that is important to the algorithm and concentrate on it. A heat-map depiction is shown in the Figure 10.

4.6 Using to Examine the EfficientNet Models

We compare the EfficientNet-B5 model to previous studies [15], [30], [32], [20], [51], [23], [24] in this section of the paper Table 4 contains an in-depth analysis of the EfficientNet-B5 model concerning multiple performance factor assessments, including accuracy, recall, and F1-score.

4.7 Discussion

The quality of life of people is significantly impacted by their dental condition. Although it is associated with everyday activities like talking, eating, and smiling, it is thought to contribute to good health [54]. The majority of young people and adults are influenced by dental cavities, an extremely common chronically harmful dental disease around the world. Acid erosion is the primary cause of dental cavities, a disease that may destroy the internal structure of teeth. Intraoral bacteria generate the majority of the acid. As a result, one of the most important tasks for dentists is to prevent dental cavities. Moreover, the treatment of cavities in teeth has frequently relied on early detection. In this study, the EfficientNets B0 to B7 models were compared to determine which one would work

Table 4. Comparing the EfficientNet-B5 model with the existing SOTA.

Ref	Year	Model	Diagnostic Technique	Accuracy	Precision	F1-Score	Recall
[52]	2023	CNN	Periapical Radiographs	94.97%	91.6%	93.5%	95.6%
[35]	2023	CNN	Panoramic Radiographs	86.05%	89.41%	-	50.67%
[37]	2023	MobileNet-V2	Periapical Radiographs	93.00%	86.00%	89.00%	89.00%
[7]	2023	GBDT, RF, LR, SVM, LSTM	Dental Images	95.19%	95.84%	93.79%	88.44%
[41]	2023	EfficientNetB0, DenseNet121, ResNet50	Panoramic Radiographs	92.00%	96.32%	91.61%	87.33%
[53]	2022	VGG, Resnet, Xception	Panoramic Radiographs	93.58%	-	92.76%	93.91%
[43]	2022	YOLO-v4 & UNet	Panoramic Radiographs	77.00%	77.00%	77.00%	77.00%
[44]	2021	CNN	Panoramic Radiographs	93.2%	-	-	96.40%
[48]	2021	DenseNet121	Panoramic Radiographs	95.7%	86.50%	89.10%	91.80%
Proposed Model	-	EfficientNet-B5	Panoramic Radiographs	98.32%	98.32%	98.37%	98.32%

best for the dental disease diagnosis. Subsequently, a technique known as Borderline SMOTE (BL-SMOTE) is implemented to address the problem related to the uneven data set. To equalize the dataset, this algorithm oversamples the categories.

Figure 1 depicts the number of dental disease samples that were divided up before the up-sampling and Figure 3 illustrates the sample allocation after the implementation of the BL-SMOTE approach. For periodontal therapy to become effective, Mao et al. [52] proposed the image masking approach for properly identifying periodontal diseases using periapical radiographs. Furthermore, their approach used a combination of fine-tuning methodologies and transfer learning to emphasize the ROI for the subsequent CNN architecture training. They eliminate the noise from the original image during the image preparation stage. Their research offered several preprocessing methods that considerably improved the model's overall performance and segmentation accuracy, including Gaussian high-pass filtering and adaptive thresholding. Furthermore, an automated procedure was created to help dentists recognize furcation involvement through images, providing a trustworthy and effective alternative for human evaluation. The trained CNN algorithm found teeth with possible illnesses with high accuracy, especially when they used the AlexNet and GoogLeNet architectures. A fully automated technique for diagnosing caries by categorizing dental regions of interest using a panoramic image was presented by Bui et al [53]. Their dataset contains the raw radiographs of 95 different people. Using a pre-trained DL model such as ResNet, VggNet, or Xception, informative characteristics were obtained from the teeth. A classification model, such as the random forest, support vector machine, or k-nearest

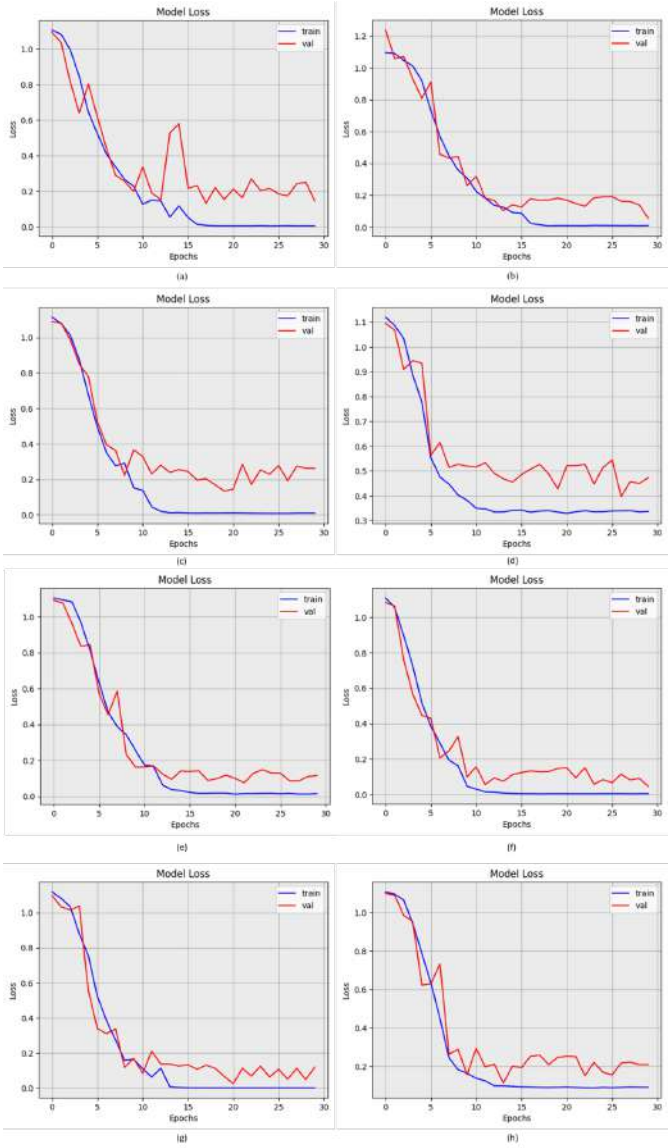

Figure 6. Loss values of the EfficientNet Models; (a) EfficientNet-B0, (b) EfficientNet-B1, (c) EfficientNet-B2, (d) EfficientNet-B3, (e) EfficientNet-B4, (f) EfficientNet-B5, (g) EfficientNet-B6, (h) EfficientNet-B7.

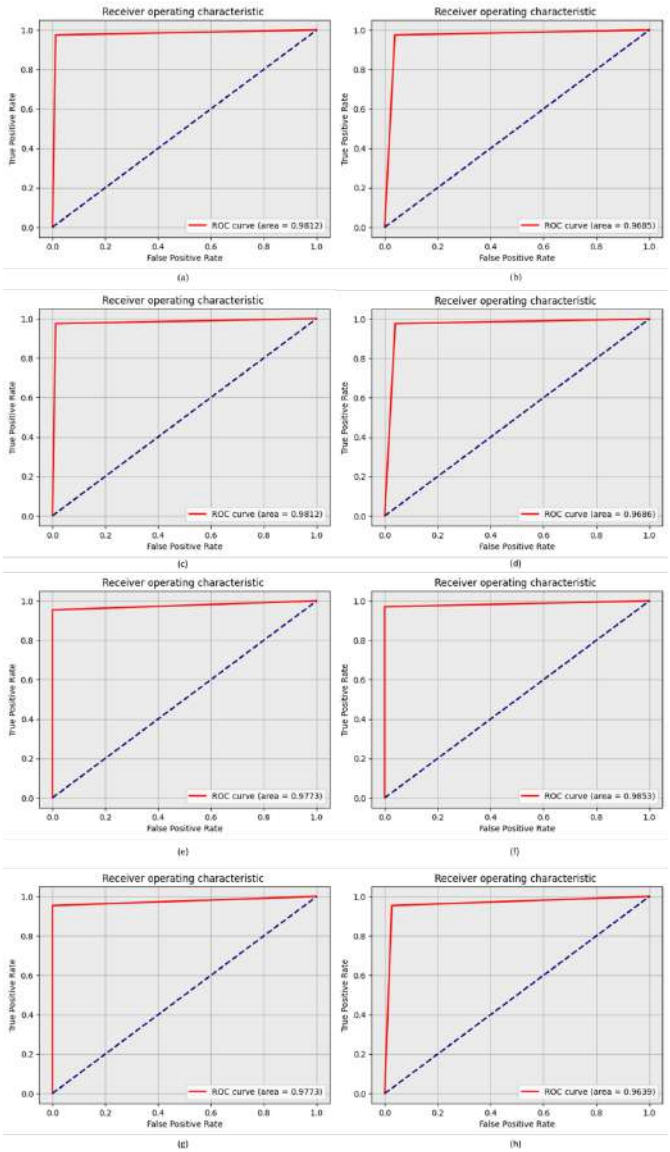

Figure 7. ROC values of the EfficientNet Models; (a) EfficientNet-B0, (b) EfficientNet-B1, (c) EfficientNet-B2, (d) EfficientNet-B3, (e) EfficientNet-B4, (f) EfficientNet-B5, (g) EfficientNet-B6, (h) EfficientNet-B7.

neighbour, learnt each extracted feature. Each classifier algorithm's prediction was regarded as a separate opinion that added to the resultant evaluation that was determined by a majority vote procedure. Their suggested approach produced results with a 93.33% specificity, 93.58% accuracy, and 93.91% sensitivity.

The results of the EfficientNet-B5 model are compared in Table 4 to the most recent study that serves as a SOTA. The EfficientNet Models, EfficientNet-B0, EfficientNet-B1, EfficientNet-B2, EfficientNet-B3, EfficientNet-B4, EfficientNet-B5, EfficientNet-B6, and EfficientNet-B7, obtained accuracies of 91.59%, 94.11%, 93.28%, 85.71%, 94.96%, 98.32%, 96.64%, and 90.76%, respectively, based on the results shown in Table 3.

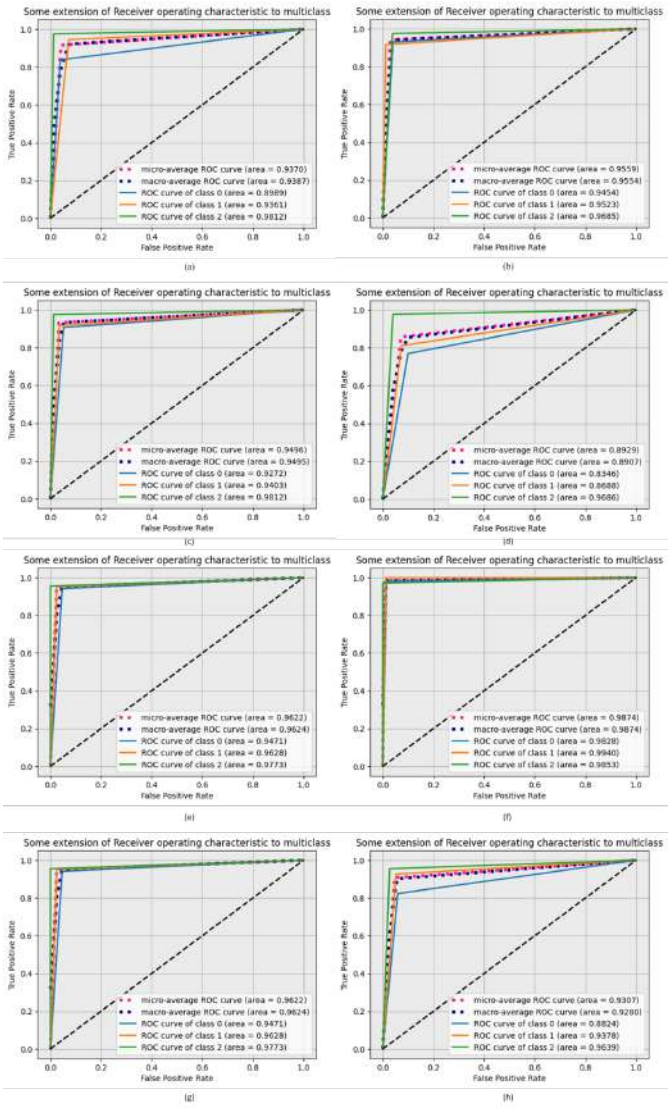

Figure 8. Extension of ROC values of the EfficientNet Models; (a) EfficientNet-B0, (b) EfficientNet-B1, (c) EfficientNet-B2, (d) EfficientNet-B3, (e) EfficientNet-B4, (f) EfficientNet-B5, (g) EfficientNet-B6, (h) EfficientNet-B7.

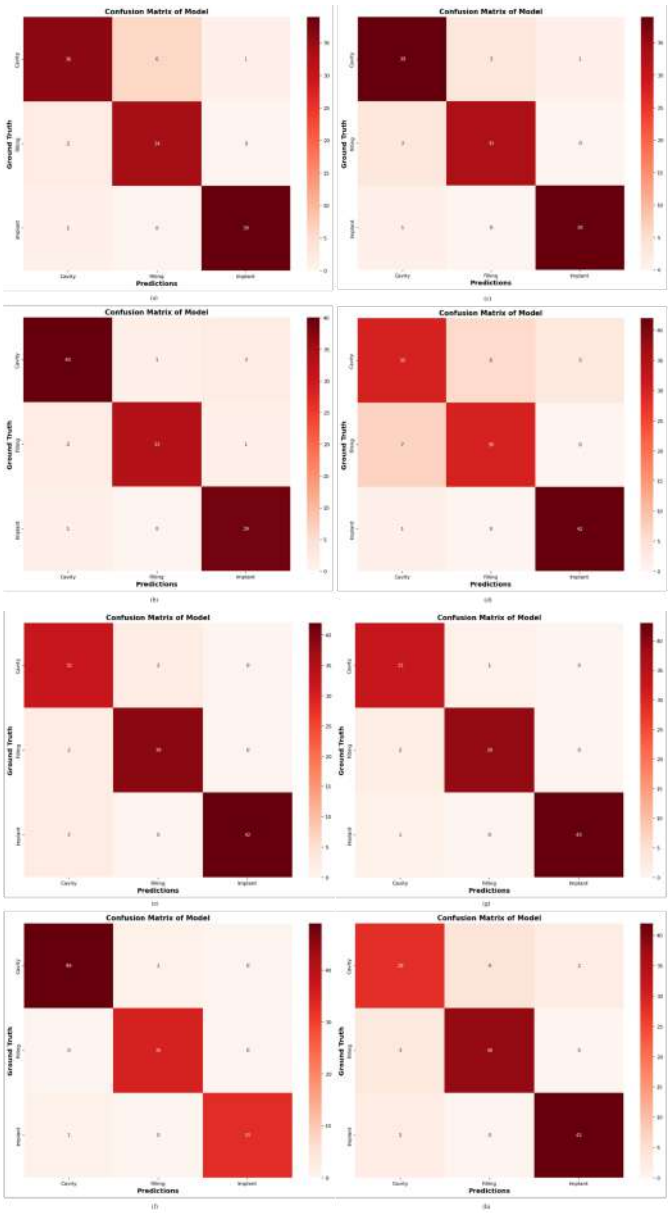

Figure 9. Confusion Matrix of the EfficientNet Models; (a) EfficientNet-B0, (b) EfficientNet-B1, (c) EfficientNet-B2, (d) EfficientNet-B3, (e) EfficientNet-B4, (f) EfficientNet-B5, (g) EfficientNet-B6, (h) EfficientNet-B7

5 Conclusion

Dental cavities analysis is one of the most often topics for today's dental healthcare research as a result of its extreme severity and incredibly high prevalence. Due to the substantial amount of cases, a rapid and efficient method for testing is essential. Dentists can identify dental diseases more quickly and correctly by applying deep learning (DL) with dental X-ray images. The X-ray images in this study have been divided into three groups: implants, fillings, and cavities. This study evaluated the performance of all of the EfficientNet variants (e.g., EfficientNets B0-B7) to determine which one is the most effective model for detecting dental disease. Additionally, we incorporated Borderline SMOTE to fix the issue with the minority classes in the dataset. The outcome was that the EfficientNet-B5

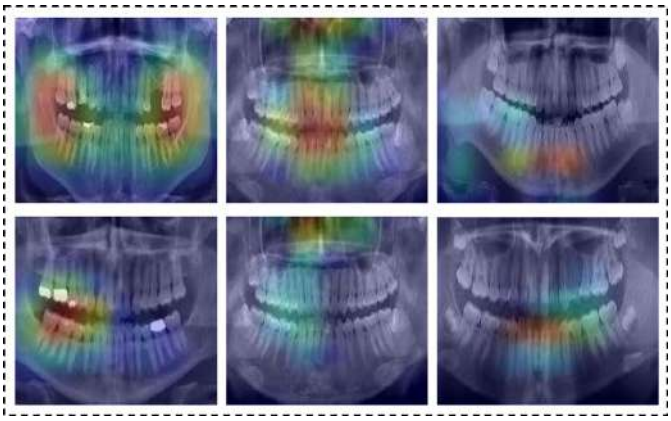

Figure 10. Dental disease visualization with Grad-CAM

model performed more effectively compared to the other EfficientNet models. The performance metrics obtained by the EfficientNet-B5 model were: F1-score, accuracy, AUC, recall, and precision; these values were: 98.37%, 98.32%, 99.21%, 98.32%, and 98.32%, respectively. EfficiencyNet-B0, EfficiencyNet-B1, EfficiencyNet-B2, EfficiencyNet-B3, EfficiencyNet-B4, EfficiencyNet-B6, and EfficiencyNet-B7 have accuracy rates of 91.59%, 94.12%, 93.28%, 85.71%, 94.96%, 96.64%, and 90.76%, respectively. The findings reveal that the EfficientNet-B5 model outperforms other EfficientNet models, hence providing dentists and other healthcare providers with substantial guidance in the identification of dental issues.

References

[1] A. M. Qilichovna, "Clinical signs when accompanied by dental diseases and metabolic syndrome," *Education Science and Innovative Ideas in the world*, vol. 39, no. 5, pp. 116–24, 2024.

[2] M. Kiarashi, H. Bayat, S. A. Shahrtash, E. A. Etajuri, M. M. Khah, N. A. Al-Shaheri, K. Nasiri, M. Esfahaniani, and S. Yasamineh, "Mesenchymal stem cell-based scaffolds in regenerative medicine of dental diseases," *Stem Cell Reviews and Reports*, vol. 20, no. 3, pp. 688–721, 2024.

[3] C. F. Husanovich, "Research on the attitude of people to the prevention of dental diseases," *European International Journal of Multidisciplinary Research and Management Studies*, vol. 4, no. 02, pp. 265–268, 2024.

[4] M. A. Hasnain, H. Malik, M. M. Asad, and F. Sherwani, "Deep learning architectures in dental diagnostics: a systematic comparison of techniques for accurate prediction of dental disease through x-ray imaging," *International Journal of Intelligent Computing and Cybernetics*, vol. 17, no. 1, pp. 161–180, 2024.

[5] J. Zarnigor, "Main role of hygienic education in the system primary prevention of dental diseases of patient," *European International Journal of Multidisciplinary Research and Management Studies*, vol. 3, no. 11, pp. 157–163, 2023.

[6] J. Zhu, Z. Chen, J. Zhao, Y. Yu, X. Li, K. Shi, F. Zhang, F. Yu, K. Shi, Z. Sun, *et al.*, "Artificial intelligence in the diagnosis of dental diseases on panoramic radiographs: a preliminary study," *BMC Oral Health*, vol. 23, no. 1, p. 358, 2023.

[7] I.-A. Kang, S. N. Njimbouom, and J.-D. Kim, "Optimal feature selection-based dental caries prediction model using machine learning for decision support system," *Bioengineering*, vol. 10, no. 2, p. 245, 2023.

[8] B. N. Muhitdinovna, "Cases of occurrence of dental diseases in workers of production enterprises," *Journal of new century innovations*, vol. 37, no. 2, pp. 68–72, 2023.

[9] Y. Zhang, F. Ye, L. Chen, F. Xu, X. Chen, H. Wu, M. Cao, Y. Li, Y. Wang, and X. Huang, "Children's dental panoramic radiographs dataset for caries segmentation and dental disease detection," *Scientific Data*, vol. 10, no. 1, p. 380, 2023.

[10] M. Mallick, S. Govindaraju, A. S. Kumar, M. Kandasamy, P. Anitha, *et al.*, "Analysis of panoramic images using deep learning for dental disease identification," in *2023 Third International Conference on Artificial Intelligence and Smart Energy (ICAIS)*, pp. 1513–1517, IEEE, 2023.

[11] S. M. D. Thumati, K. Dhanya, H. Sathish, K. S. Madan, and S. Rani, "A comparative study on the working of gnn and cnn on panoramic x-rays in prediction of dental diseases," in *2023 8th International Conference on Communication and Electronics Systems (ICCES)*, pp. 755–762, IEEE, 2023.

[12] P. Ntovas, S. Michou, A. Benetti, A. Bakhshandeh, K. Ekstrand, C. Rahiotis, and A. Kakaboura, "Occlusal caries detection on 3d models obtained with an intraoral scanner. a validation study," *Journal of Dentistry*, vol. 131, p. 104457, 2023.

[13] Z. Metzger, D. G. Colson, P. Bown, T. Weihard, I. Baresel, and T. Nolting, "Reflected near-infrared light versus bitewing radiography for the detection of proximal caries: A multicenter prospective clinical study conducted in private practices," *Journal of Dentistry*, vol. 116, p. 103861, 2022.

[14] J. Gomez, "Detection and diagnosis of the early caries lesion," *BMC oral health*, vol. 15, no. Suppl 1, p. S3, 2015.

[15] A. Ossowska, A. Kusiak, and D. Świetlik, "Artificial intelligence in dentistry—narrative review," *International journal of environmental research and public health*, vol. 19, no. 6, p. 3449, 2022.

[16] M. Abdinian, S. M. Razavi, R. Faghihian, A. A. Samety, and E. Faghihian, "Accuracy of digital bitewing radiography versus different views of digital panoramic radiography for detection of proximal caries," *Journal of Dentistry (Tehran, Iran)*, vol. 12, no. 4, p. 290, 2015.

[17] M. A. Hasnain, S. Ali, H. Malik, M. Irfan, and M. S. Maqbool, "Deep learning-based classification of dental disease using x-rays," *Journal of Computing & Biomedical Informatics*, vol. 5, no. 01, pp. 82–95, 2023.

[18] A. Terlemez, M. Tassoker, M. Kizilcakaya, and M. Gulec, "Comparison of cone-beam computed tomography and panoramic radiography in the evaluation of maxillary sinus pathology related to maxillary posterior teeth: Do apical lesions increase the risk of maxillary sinus pathology?," *Imaging science in dentistry*, vol. 49, no. 2, p. 115, 2019.

[19] J. Ullinger and T. Loewen, "Dental disease," *The Routledge Handbook of Paleopathology*, pp. 360–378, 2022.

[20] D. L. Duong, M. H. Kabir, and R. F. Kuo, "Automated caries detection with smartphone color photography using machine learning," *Health informatics journal*, vol. 27, no. 2, p. 14604582211007530, 2021.

[21] E. Sivari, G. B. Senirkentli, E. Bostanci, M. S. Guzel, K. Acici, and T. Asuroglu, "Deep learning in diagnosis of dental anomalies and diseases: A systematic review," *Diagnostics*, vol. 13, no. 15, p. 2512, 2023.

[22] V. Gulshan, L. Peng, M. Coram, M. C. Stumpe, D. Wu, A. Narayanaswamy, S. Venugopalan, K. Widner, T. Madams, J. Cuadros, *et al.*, "Development and validation of a deep learning algorithm for detection of diabetic retinopathy in retinal fundus photographs," *jama*, vol. 316, no. 22, pp. 2402–2410, 2016.

[23] A. Esteva, B. Kuprel, R. A. Novoa, J. Ko, S. M. Swetter, H. M. Blau, and S. Thrun, "Dermatologist-level classification of skin cancer with deep neural networks," *nature*, vol. 542, no. 7639, pp. 115–118, 2017.

[24] M. Kallenberg, K. Petersen, M. Nielsen, A. Y. Ng, P. Diao, C. Igel, C. M. Vachon, K. Holland, R. R. Winkel, N. Karssemeijer, *et al.*, "Unsupervised deep learning applied to breast density segmentation and mammographic risk scoring," *IEEE transactions on medical imaging*, vol. 35, no. 5, pp. 1322–1331, 2016.

[25] H. Lee, M. Park, and J. Kim, "Cephalometric landmark detection in dental x-ray images using convolutional neural networks," in *Medical imaging 2017: Computer-aided diagnosis*, vol. 10134, pp. 494–499, SPIE, 2017.

[26] A. Y. Hannun, P. Rajpurkar, M. Haghpanahi, G. H. Tison, C. Bourn, M. P. Turakhia, and A. Y. Ng, "Cardiologist-level arrhythmia detection and classification in ambulatory electrocardiograms using a deep neural network," *Nature medicine*, vol. 25, no. 1, pp. 65–69, 2019.

[27] G. Yao, T. Lei, and J. Zhong, "A review of convolutional-neural-network-based action recognition," *Pattern Recognition Letters*, vol. 118, pp. 14–22, 2019.

[28] A. Dhillon and G. K. Verma, "Convolutional neural network: a review of models, methodologies and applications to object detection," *Progress in Artificial Intelligence*, vol. 9, no. 2, pp. 85–112, 2020.

[29] R. Yamashita, M. Nishio, R. K. G. Do, and K. Togashi, "Convolutional neural networks: an overview and application in radiology," *Insights into imaging*, vol. 9, pp. 611–629, 2018.

[30] J.-H. Lee, D.-H. Kim, S.-N. Jeong, and S.-H. Choi, "Detection and diagnosis of dental caries using a deep learning-based convolutional neural network algorithm," *Journal of dentistry*, vol. 77, pp. 106–111, 2018.

[31] H. Mohammad-Rahimi, S. R. Motamedian, M. H. Rohban, J. Krois, S. E. Uribe, E. Mahmoudinia, R. Rokhshad, M. Nadimi, and F. Schwendicke, "Deep learning for caries detection: A systematic review," *Journal of Dentistry*, vol. 122, p. 104115, 2022.

[32] J.-H. Lee, D.-h. Kim, S.-N. Jeong, and S.-H. Choi, "Diagnosis and prediction of periodontally compromised teeth using a deep learning-based convolutional neural network algorithm," *Journal of periodontal & implant science*, vol. 48, no. 2, pp. 114–123, 2018.

[33] Z. Ali, W. Tiberti, A. Marotta, and D. Cassioli, "Empowering network security: Bert transformer learning approach and mlp for intrusion detection in imbalanced network traffic," *IEEE Access*, pp. 1–1, 2024.

[34] S. Kalita, R. Singh, A. I. Abidi, H. Sawhney, and G. Noida, "Dental caries grade classification based on improved very deep convolutional neural network," *Journal of Data Acquisition and Processing*, vol. 38, no. 2, p. 2794, 2023.

[35] A. Haghanifar, M. M. Majdabadi, S. Haghanifar, Y. Choi, and S.-B. Ko, "Paxnet: Tooth segmentation and dental caries detection in panoramic x-ray using ensemble transfer learning and capsule classifier," *Multimedia Tools and Applications*, vol. 82, no. 18, pp. 27659–27679, 2023.

[36] I. D. S. Chen, C.-M. Yang, M.-J. Chen, M.-C. Chen, R.-M. Weng, and C.-H. Yeh, "Deep learning-based recognition of periodontitis and dental caries in dental x-ray images," *Bioengineering*, vol. 10, no. 8, p. 911, 2023.

[37] A. Fatima, I. Shafi, H. Afzal, K. Mahmood, I. d. l. T. Díez, V. Lipari, J. B. Ballester, and I. Ashraf, "Deep learning-based multiclass instance segmentation for dental lesion detection," in *Healthcare*, vol. 11, p. 347, MDPI, 2023.

[38] W. Panyarak, K. Wantanajittikul, W. Suttapak, A. Charuakkra, and S. Prapayasatok, "Feasibility of deep learning for dental caries classification in bitewing radiographs based on the iccms™ radiographic scoring system," *Oral Surgery, Oral Medicine, Oral Pathology and Oral Radiology*, vol. 135, no. 2, pp. 272–281, 2023.

[39] B. Dayı, H. Üzen, İ. B. Çiçek, and Ş. B. Duman, "A novel deep learning-based approach for segmentation of different type caries lesions on panoramic radiographs," *Diagnostics*, vol. 13, no. 2, p. 202, 2023.

[40] A. S. A.-M. Al-Ghamdi, M. Ragab, S. A. AlGhamdi, A. H. Asseri, R. F. Mansour, and D. Koundal, "Detection of dental diseases through x-ray images using neural search architecture network," *Computational Intelligence and Neuroscience*, vol. 2022, no. 1, p. 3500552, 2022.

[41] F. Oztekin, O. Katar, F. Sadak, M. Yildirim, H. Cakar, M. Aydogan, Z. Ozpolat, T. Talo Yildirim, O. Yildirim, O. Faust, *et al.*, "An explainable deep learning model to prediction dental caries using panoramic radiograph images," *Diagnostics*, vol. 13, no. 2, p. 226, 2023.

[42] A. Karaoglu, C. Ozcan, A. Pekince, and Y. Yasa, "Numbering teeth in panoramic images: A novel method based on deep learning and heuristic algorithm," *Engineering Science and Technology, an International Journal*, vol. 37, p. 101316, 2023.

[43] L. Jiang, D. Chen, Z. Cao, F. Wu, H. Zhu, and F. Zhu, "A two-stage deep learning architecture for radiographic staging of periodontal bone loss," *BMC Oral Health*, vol. 22, no. 1, p. 106, 2022.

[44] C. Muramatsu, T. Morishita, R. Takahashi, T. Hayashi, W. Nishiyama, Y. Ariji, X. Zhou, T. Hara, A. Katsumata, E. Ariji, *et al.*, "Tooth detection and classification on panoramic radiographs for automatic dental chart filing: improved classification by multi-sized input data," *Oral Radiology*, vol. 37, pp. 13–19, 2021.

[45] M. P. Muresan, A. R. Barbura, and S. Nedevschi, "Teeth detection and dental problem classification in panoramic x-ray images using deep learning and image processing techniques," in *2020 IEEE 16th International Conference on Intelligent Computer Communication and Processing (ICCP)*, pp. 457–463, IEEE, 2020.

[46] I.-A. Kang, S. Ngnamsie Njimbouom, K.-O. Lee, and J.-D. Kim, "Dcp: prediction of dental caries using machine learning in personalized medicine," *Applied Sciences*, vol. 12, no. 6, p. 3043, 2022.

[47] S. Ngnamsie Njimbouom, K. Lee, and J.-D. Kim, "Mmdcp: multi-modal dental caries prediction for decision support system using deep learning," *International Journal of Environmental Research and Public Health*, vol. 19, no. 17, p. 10928, 2022.

[48] L. Lian, T. Zhu, F. Zhu, and H. Zhu, "Deep learning for caries detection and classification," *Diagnostics*, vol. 11, no. 9, p. 1672, 2021.

[49] H. Han, W.-Y. Wang, and B.-H. Mao, "Borderline-smote: a new over-sampling method in imbalanced data sets learning," in *International conference on intelligent computing*, pp. 878–887, Springer, 2005.

[50] M. Tan, "Efficientnet: Rethinking model scaling for convolutional neural networks," *arXiv preprint arXiv:1905.11946*, 2019.

[51] J. E. Sklan, A. J. Plassard, D. Fabbri, and B. A. Landman, "Toward content-based image retrieval with deep convolutional neural networks," in *Medical Imaging 2015:*

Biomedical Applications in Molecular, Structural, and Functional Imaging, vol. 9417, pp. 633–638, SPIE, 2015.

[52] Y.-C. Mao, Y.-C. Huang, T.-Y. Chen, K.-C. Li, Y.-J. Lin, Y.-L. Liu, H.-R. Yan, Y.-J. Yang, C.-A. Chen, S.-L. Chen, *et al.*, "Deep learning for dental diagnosis: A novel approach to furcation involvement detection on periapical radiographs," *Bioengineering*, vol. 10, no. 7, p. 802, 2023.

[53] T. H. Bui, K. Hamamoto, and M. P. Paing, "Automated caries screening using ensemble deep learning on panoramic radiographs," *Entropy*, vol. 24, no. 10, p. 1358, 2022.

[54] R. Baiju, E. Peter, N. Varghese, and R. Sivaram, "Oral health and quality of life: current concepts," *Journal of clinical and diagnostic research: JCDR*, vol. 11, no. 6, p. ZE21, 2017.